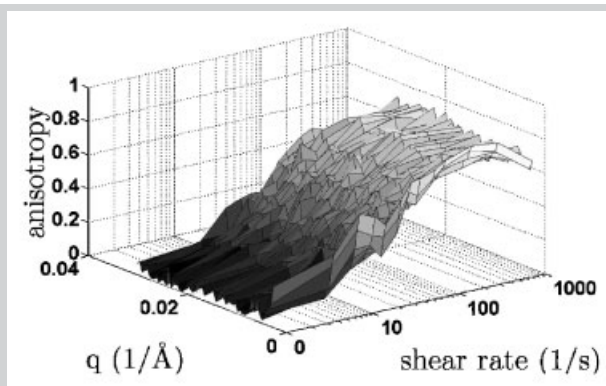


Summary: Shear-induced orientation of nanoparticles in poly(ethylene oxide)/Laponite RD hydrogels has been investigated by small angle neutron scattering (SANS). As temperature is reduced, anisotropy develops at lower shear rates. The two-correlation length Debye–Anderson–Brumberger (DAB) model provides a good fit to the experimental data. The deduced short-range correlation length (≈ 5 nm) is observed to increase with shear. The long-range correlation length (≈ 50 nm) shows a strong directional dependence, and decreases when shear is applied. The relative contribution of long-range order to the SANS intensity is observed to increase with shear and decrease with temperature.



SANS anisotropy $|(I_y - I_x)/(I_y + I_x)|$ as a function of shear rate and q at 2°C .

Effect of Temperature on Shear-Induced Anisotropic Structure in Polymer Clay Hydrogels

Jun Li,^{*1,2} Jun Jiang,³ Chunhua Li,³ Min Y. Lin,^a Steven A. Schwarz,^{*1} Miriam H. Rafailovich,³ Jonathan Sokolov³

¹Department of Physics, Queens College, City University of New York, Flushing, New York 11367, USA

Fax: (+1) 718 997 3349; E-mail: jli22@qc.cuny.edu; steven.schwarz@qc.cuny.edu

²Physics Ph. D. Program, Graduate Center, City University of New York, New York 10016, USA

³Department of Materials Science and Engineering, SUNY Stony Brook, Stony Brook, New York 11794, USA

Received: June 27, 2006; Revised: August 16, 2006; Accepted: August 17, 2006; DOI: 10.1002/marc.200600438

Keywords: clay; composite; hydrogels; neutron scattering; orientation; polyethylene

Introduction

Layered silicate-based nanocomposite materials have attracted much interest recently, as they present a cost-effective approach to improve the mechanical properties, flame retardance, and thermal stability of polymer systems.^[1,2] The enhanced material properties depend not only on the dispersion of the filler, but also on the orientation of the high aspect ratio nanoparticles. Laponite RD (LRD), a synthetic clay, can disperse in water as disk-shaped particles, 30 nm in diameter and 1 nm in thickness. Each platelet displays more negative charge on its face, and less negative charge at the edge. The electrostatic interaction between platelets may lead to a house of cards structure described by van Olphen.^[3] Clay

platelets will orient under shear, and butterfly type patterning has been shown in light scattering experiments for colloids.^[4]

Upon introduction of polymer to the clay aqueous solution, polymer chains will interact with the clay platelets and may be adsorbed on the surface of clay platelets. With contrast variation small angle neutron scattering (SANS) measurement, Nelson and Cosgrove showed that the addition of poly(ethylene oxide) (PEO) to a Laponite aqueous solution will cause the clay platelets to be enveloped by PEO, leading to a thickness change on each face of about 1.5 nm and a radius change in the range of 1.5–4.5 nm.^[5] Under shear, the clay platelets may orient and thus stretch the polymer chains bridging the platelets; therefore, an anisotropic shear-induced structure can be expected. Schmidt and coworkers have observed the development of anisotropic neutron scattering and light scattering patterns for the PEO/Laponite aqueous solution under shear.^[6,7] Shibayama et al. have observed that clay

^a Present address: P.O. Box 3862, Gaithersburg, Maryland 20885, USA. Previously at the National Institute for Standards and Technology.

platelets are strongly tethered by poly(*N*-isopropylacrylamide) (PNIPA) chains.^[8] A butterfly SANS pattern develops when the sample is stretched. All these experiments have been performed at room temperature; the effect of temperature has not yet been revealed.

When temperature increases, the rotational Brownian motion of clay platelets acts in opposition to shear-induced platelet orientation. Perrin and Jerrard showed that the rotational diffusion constant for platelet-like particles increases in proportion to temperature.^[9,10] At the same time, stretched polymer chains that bridge adjacent platelets will relax faster at higher temperature, again acting in opposition to shear-induced anisotropy. In this regard, Doi and Edward derived that the rotational relaxation time of polymer is inversely proportional to the temperature.^[11] Temperature also affects PEO stability in aqueous solvent.^[12–14] The attractive force between the PEO-covered surfaces in water has been predicted to be related to the temperature-dependent solubility of PEO in water.^[12] As temperature increases, hydrogen bonds are more easily broken, decreasing the solvency of PEO in water, and consequently decreasing the layer thickness adsorbed to the particle.^[13] At the same time, a higher temperature enhances the bridging interaction of polymer chains on adjacent particles,^[14] which could aid the development of anisotropy. To elucidate the competing effects of stabilization, Brownian rotational motion, and relaxation, we examine here the evolution of shear-induced structure in PEO LRD hydrogels at different temperatures.

Experimental Part

Samples were composed of 3.0 wt.-% LRD (Southern Clay), deuterium oxide (D₂O) (99.7%, Cambridge), and 1.5 wt.-% PEO (Aldrich) with $\bar{M}_w = 900\,000$. LRD was added to D₂O and the solution was ultrasonicated for several hours and left still for about 10 h to assist the exfoliation of LRD. After the solution became transparent, PEO was added and the solution was magnetically stirred. It took about two weeks for the system to become homogeneous.

SANS experiments were performed at the NG3 and NG7 SANS instruments of the Center for Neutron Research, National Institute of Standards and Technology. The Boulder shear cell used in the dynamic SANS experiments has a Couette geometry with i.d. of 60.952 mm. The gap is 0.45 mm, giving a total path length of 0.90 mm through the sample. The incident neutron beam is parallel to the shear gradient. The incident wavelength, λ , was 6 Å, and the scattering wave vector, q , covered range for the dynamic SANS experiments was 0.0029–0.0437 Å⁻¹. The temperature of the sample was set at 2, 25, and 50 °C. At each temperature, the shear rate was increased from 0 to 1 000 s⁻¹ in 14 steps. Then, the shear cell sat at rest to monitor the relaxation of the system. When the temperature was changed, a new sample was employed in order to avoid remnant shear effects. Static SANS was performed in the low q range (0.0021–0.0418 Å⁻¹) at temperatures of 10, 20, 30, and 40 °C.

Results and Discussion

Two-dimensional scattering patterns of dynamic SANS measurements at different temperatures and shear rates are shown in Figure 1. At 2 °C, anisotropy is apparent in the 2D image when the shear rate is 50 s⁻¹, while a similar pattern appears at 25 °C with a shear rate of 100 s⁻¹, and at 200 s⁻¹ when the temperature is 50 °C. After the shear rate reached 1 000 s⁻¹, the shear cell was stopped in order to monitor relaxation of the anisotropy. A scattering pattern was obtained at rest, as shown at the far right of the figure, within two minutes of the cessation of motion. At 2 and 25 °C, some anisotropy remains, while at 50 °C, the sample has become isotropic.

To elucidate the influence of temperature to anisotropy, we calculate the anisotropy $|(I_y - I_x)/(I_y + I_x)|$ for different q at each shear rate. I_x and I_y correspond to the SANS intensity from sectors around 0° (parallel to the flow) and 90° (perpendicular to the flow) in a range of 10°, respectively. At 2 °C, the anisotropy as a function of q and shear rate is shown in Figure 2(a). The figure indicates that the change in the anisotropy is mainly dominated by the shear rate. Therefore, the average anisotropies were calculated by integrating over the whole q range for each shear rate. As shown in Figure 2(b), anisotropy is more sensitive to shear rate as the temperature decreases. As noted previously, the anisotropic structure is generated by both the orientation of clay platelets and the stretch of polymer chains. At lower temperature, a smaller threshold shear rate is required to orient the clay platelets and stretch the polymer chains that bridge the clay platelets.

According to Hammouda et al., there exist two correlation lengths in the PEO/water system.^[15] We also observed a drop off in the low q region of the SANS intensity curves. The curves can be well fit by the two-correlation length Debye–Anderson–Brumberger (DAB) model:^[16]

$$I = A_1/(1 + q^2R_1^2)^2 + A_2 \exp(-q^2R_2^2/4) \quad (1)$$

where A_1 and A_2 are fitting parameters that depend on incident beam intensity and sample contrast; R_1 represents a short-range correlation length, and R_2 represents the correlation length for a larger inhomogeneous region. The correlation function is

$$\gamma(r) = f \exp(-r/R_1) + (1 - f) \exp(-r^2/R_2^2) \quad (2)$$

where f is given by

$$f = A_1 / \left[A_1 + \frac{8}{\sqrt{\pi}} \left(\frac{R_1}{R_2} \right)^3 A_2 \right] \quad (3)$$

Here f indicates the weight of short-range correlation in the total correlation, so that $1 - f$ represents the weight of long-

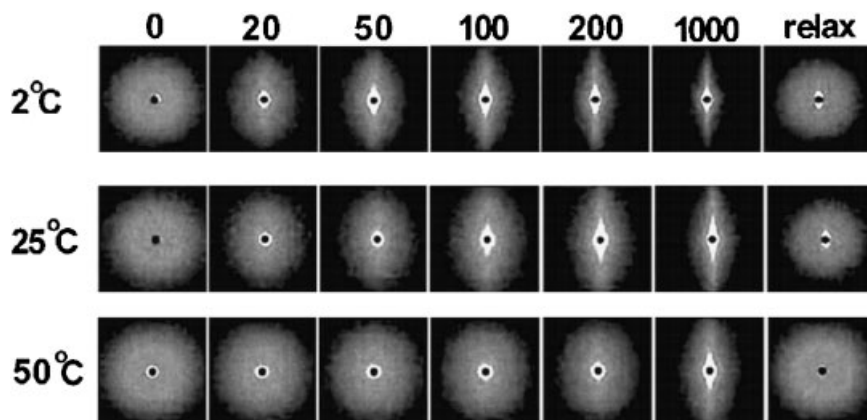


Figure 1. Two-dimensional SANS scattering patterns at three temperatures, with shear rates (s^{-1}). The patterns at the far right were obtained immediately after the application of highest shear, with the Couette cell at rest.

range correlation. When $f=1$, the two-correlation length DAB model reduces to one-correlation length DAB model.

We built a macro in Excel Solver and applied the two-correlation length DAB model to fit the circular average

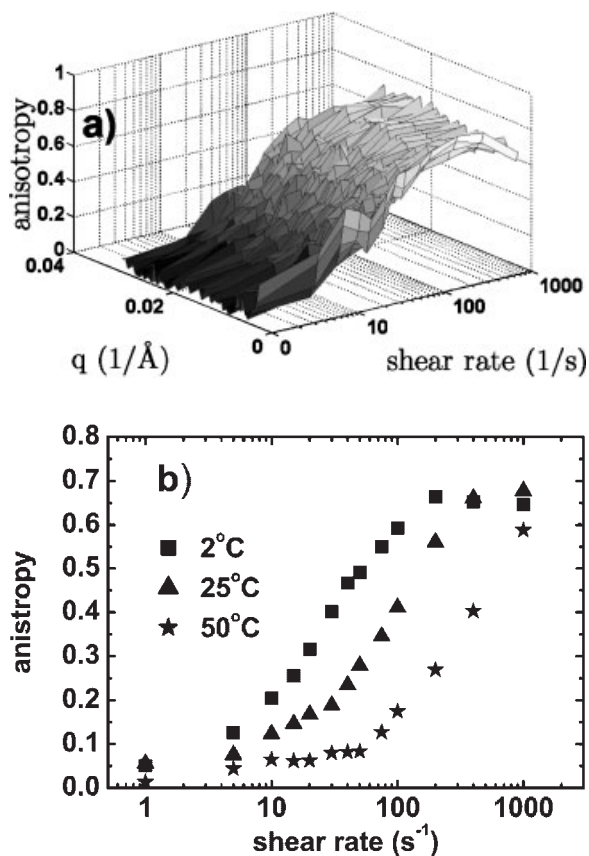


Figure 2. (a) SANS anisotropy $|(I_y - I_x)/(I_y + I_x)|$ as a function of shear rate and q at 2°C ; (b) anisotropy averaged over the entire q range as a function of shear rate at three different temperatures as indicated.

static SANS data at different temperatures. Two of the fits are shown in Figure 3. We clearly see a drop off near the low q end, indicating a long-range correlation. The parameter values derived from the fits are shown in Table 1. As temperature increases from 10 to 40°C at zero shear, the short-range correlation length drops from 4.7 to 3.9 nm, but the long-range correlation length increases from about 87 to 117 nm. This is opposite to the trend observed in a pure PEO aqueous solution.^[5] The relative weight of the long-range correlation, $1-f$, decreases as temperature increases. It is likely that the short-range correlation is associated with a domain composed of a clay platelet and adhered polymer, while the long-range correlation represents the interaction between different domains. The short-range correlation length of ≈ 4 nm matches the thickness of clay platelet and polymer absorbed to it which has been observed by TEM,^[17] and also agrees with the thickness

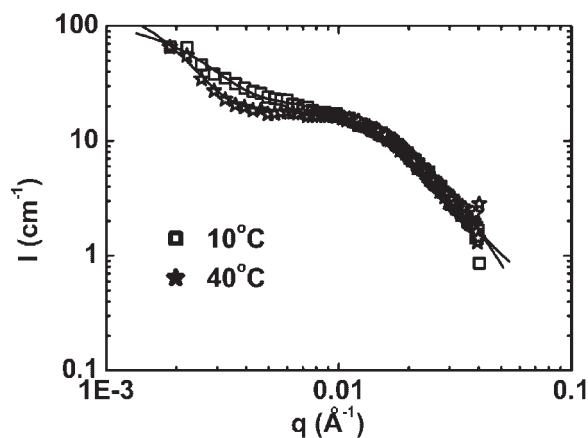


Figure 3. Static SANS intensity versus q at 10 and 40°C . Solid lines show the fits obtained by the DAB model for the parameters given in Table 1.

Table 1. DAB fitting results for static SANS data.

Temperature	R_1	R_2	$1-f$
°C	nm	nm	
10	4.7	87	0.0025
20	4.7	88	0.0022
30	4.3	106	0.0015
40	3.9	117	0.0014

shown by Nelson and Cosgrove on a Laponite platelet wrapped by PEO.^[5] In contrast, the observed long-range correlation length of ≈ 100 nm is close to the mesh size in the hydrogel networks shown in TEM, and is similar to the distance between polymer-covered clay rich domains observed by small angle X-ray scattering (SAXS).^[17,18]

The temperature dependence of the correlation lengths is consistent with the effects of steric repulsion and bridging

interaction described by Shay and coworkers.^[14] When temperature increases, solvency of PEO in water decreases, and grafted PEO chains shrink toward the particle surface. As the short-range correlation length is associated with the thickness of the PEO/clay domain, it should, therefore, decrease at higher temperature. Furthermore, increased bridging interactions at higher temperature are likely to be related to the increase in the long-range correlation length.

The influence of shear rate is revealed by applying the two-correlation DAB model to the dynamic SANS data. As shown in Figure 4(a) and 4(b), the short-range correlation length is in the range of several nanometers. As shear rate increases, the short-range correlation length tends to increase and the threshold shear rate is smaller at lower temperature. The increase of length may indicate shear extension of the polymer adhered to the clay platelets. At lower temperatures, a smaller energy is needed to deform the domain and, therefore, a smaller shear force is required to induce anisotropy.

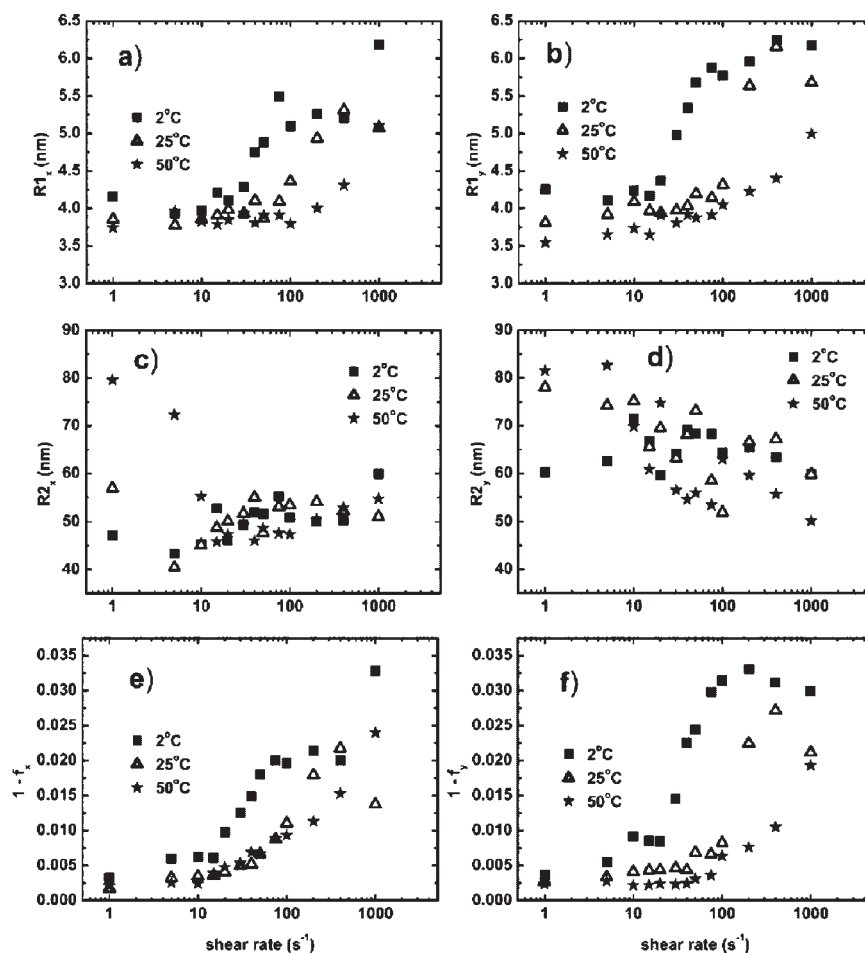


Figure 4. Application of the DAB model to the dynamic SANS data averaged over a 10° range in the x (parallel) and y (perpendicular) directions. (a) and (b): Short-range correlation lengths parallel and perpendicular to the shear flow direction; (c) and (d): corresponding long-range correlation lengths; (e) and (f): corresponding relative strengths of long-range correlation $1-f$.

As shown in Figure 4(c) and 4(d), the long-range correlation length is in the range of 40–100 nm. In the x -direction, parallel to the direction of shear flow, this length drops rapidly from its static value, listed in Table 1, as shear is applied. The drop off with shear is slowest at 50 °C, as expected due to inhibition of platelet orientation by Brownian rotational motion at high temperature. In the perpendicular y -direction, only a small reduction in the long-range correlation length is observed as shear is applied, consistent with a small rotation of platelets in a direction perpendicular to shear flow. In Figure 4(e) and 4(f), the relative strength of long-range correlation, $1 - f$, increases as the shear rate rises. Furthermore, $1 - f$ begins to rise at a lower shear rate when temperature is lower. The presence of long-range order is clearly correlated with the development of anisotropy, as evidenced by the similarity in the plot of anisotropy versus shear rate in Figure 2(b).

Conclusion

An application of the two-correlation length DAB model to static and dynamic SANS data for the PEO/Laponite hydrogels at various temperatures reveals significant trends. The short-correlation length, associated with polymer adhered to an individual platelet, decreases with temperature as the attached PEO chains shrink toward the particle surface owing to decreased solubility. At zero shear, the long correlation length, associated with polymer chains bridging different clay platelets, increases with temperature while the strength of long-range correlation decreases. The increased long correlation length is likely to be related to enhance bridging interactions. As the shear rate increases, the short-range correlation length increases, and is attributed to the extension of adhered polymer chains. At low shear rate, the long-range correlation length drops quickly with shear in the flow direction, especially at the lower temperatures, but is less affected in the perpendicular direction. As the shear rate increases, the long-range correlation length in both directions hovers around 60 nm. However, the relative strength of long-range correlation generally increases with shear rate, and is well correlated with the development of anisotropy at the

corresponding temperature, as observed in the SANS scattering patterns. These patterns also reveal rapid relaxation of anisotropy at high temperature. Extension to other concentrations and molecular weights will be reported in a forthcoming publication.

Acknowledgements: We acknowledge the support of the National Institute of Standards and Technology, U. S. Department of Commerce, in providing the neutron research facilities used in this work as well as support by the NSF MRSEC (DMR9632525) and PSC-CUNY programs.

- [1] M. Alexandre, Ph. Dubois, *Mater. Sci. Eng.* **2000**, *28*, 1.
- [2] M. Alexandre, G. Beyer, C. Henrist, R. Cloots, A. Rulmont, R. Jerome, Ph. Dubois, *Macromol. Rapid Commun.* **2001**, *22*, 643.
- [3] H. van Olphen, "An Introduction to Clay Colloid Chemistry", John Wiley and Sons, New York 1977.
- [4] F. Pignon, A. Magnin, J. M. Piau, *Phys. Rev. Lett.* **1997**, *79*, 4689.
- [5] A. Nelson, T. Cosgrove, *Langmuir* **2004**, *20*, 2298.
- [6] S. Lin-Gibson, H. Kim, G. Schmidt, C. C. Han, E. K. Hobbie, *J. Colloid Interf. Sci.* **2004**, *274*, 515.
- [7] G. Schmidt, A. I. Nakatani, P. D. Butler, C. C. Han, *Macromolecules* **2002**, *35*, 4725.
- [8] M. Shibayama, T. Karino, S. Miyazaki, S. Okabe, T. Takehisa, K. Haraguchi, *Macromolecules* **2005**, *38*, 10772.
- [9] F. Perrin, *J. Phys. Radium* **1934**, *5*, 497.
- [10] H. G. Jerrard, *Chem. Rev.* **1959**, *59*, 345.
- [11] M. Doi, S. F. Edward, "The Theory of Polymer Dynamics", Oxford University Press, 1986.
- [12] M. Bjorling, *Macromolecules* **1992**, *25*, 3956.
- [13] W. Liang, Th. F. Tadros, P. F. Luckham, *Langmuir* **1993**, *9*, 2077.
- [14] J. S. Shay, S. R. Raghavan, S. A. Khan, *J. Rheol.* **2001**, *45*, 913.
- [15] B. Hammouda, D. Ho, S. Kline, *Macromolecules* **2002**, *35*, 8578.
- [16] P. Debye, H. R. Anderson, H. Brumberger, *J. Appl. Phys.* **1957**, *28*, 679.
- [17] E. Loizhou, P. Butler, L. Porcar, E. Kesselman, Y. Zalman, A. Dundigalla, G. Schmidt, *Macromolecules* **2005**, *38*, 2047.
- [18] A. Dundigalla, S. Lin-Gibson, V. Ferreiro, M. M. Malwitz, G. Schmidt, *Macromol. Rapid Commun.* **2005**, *26*, 143.